microbial biotechnology

Microbial Biotechnology (2012) **5**(6), 738–752 doi:10.1111/j.1751-7915.2012.00364.x

Microbial community structure and dynamics in anaerobic fluidized-bed and granular sludge-bed reactors: influence of operational temperature and reactor configuration

Katarzyna Bialek,[1] Amit Kumar,[2,3] Thérèse Mahony,[1] Piet N. L. Lens[2] and Vincent O' Flaherty[1]*

[1]*Microbial Ecology Laboratory, Microbiology, School of Natural Sciences and Ryan Institute, National University of Ireland, Galway, Ireland.*

[2]*Department of Environmental Engineering and Water Technology, UNESCO-IHE, Delft, The Netherlands.*

[3]*Ryan Institute, National University of Ireland, Galway, Ireland.*

Summary

Methanogenic community structure and dynamics were investigated in two different, replicated anaerobic wastewater treatment reactor configurations [inverted fluidized bed (IFB) and expanded granular sludge bed (EGSB)] treating synthetic dairy wastewater, during operating temperature transitions from 37°C to 25°C, and from 25°C to 15°C, over a 430-day trial. Non-metric multidimensional scaling (NMS) and moving-window analyses, based on quantitative real-time PCR data, along with denaturing gradient gel electrophoresis (DGGE) profiling, demonstrated that the methanogenic communities developed in a different manner in these reactor configurations. A comparable level of performance was recorded for both systems at 37°C and 25°C, but a more dynamic and diverse microbial community in the IFB reactors supported better stability and adaptative capacity towards low temperature operation. The emergence and maintenance of particular bacterial genotypes (phylum *Firmicutes* and *Bacteroidetes*) was associated with efficient protein hydrolysis in the IFB, while protein hydrolysis was inefficient in the EGSB. A significant community shift from a *Methanobacteriales* and *Methanosaetaceae* towards a *Methanomicrobiales*-predominated community was demonstrated during operation at 15°C in both reactor configurations.

Received 12 April, 2012; revised 6 July, 2012; accepted 6 August, 2012. *For correspondence. E-mail vincent.oflaherty@nuigalway.ie; Tel. (+353) 91 493734; Fax (+353) 91 494598.

Introduction

Bioenergy production from waste streams is a key component in the global development of sustainable energy sources (Demirel *et al*., 2010). Indeed, anaerobic digestion (AD) is poised to replace aerobic microbiological treatments as the core process of waste-to-energy technologies for enhanced sustainability in the coming decades (Verstraete and Gusseme, 2011). During AD, organic substrates are sequentially degraded by fermentative and acetogenic bacteria to simple precursor compounds, such as acetate, H_2/CO_2, formate and methanol, from which methanogenic *Archaea* produce a methane-rich biogas. Temperature can influence the rate and path of carbon flow during methanogenesis by affecting the activity of particular microbial groups and the structure of the microbial consortia (O'Reilly *et al*., 2009; McKeown *et al*., 2009a; Siggins *et al*., 2011).

Low-temperature AD (LTAD) has emerged as an economically attractive waste treatment strategy, which confers considerable advantages over conventional mesophilic (~ 30°C) and thermophilic (~ 55°C) treatments, primarily due to the capacity to treat the wide variety of cool, dilute wastewaters, previously considered as not suitable for AD (McKeown *et al*., 2012). LTAD has been successfully applied at laboratory- and pilot-scale, using a variety of reactor types, for the treatment of a broad range of wastewaters (for example, Lettinga *et al*., 2001; Collins *et al*., 2003; 2006; McHugh *et al*., 2004; Syutsubo *et al*., 2008; Bergamo *et al*., 2009; McKeown *et al*., 2012). LTAD is an attractive technology because the process is stable, simple to operate and requires very low energy input. Improved reactor designs enable high rates of methanogenic conversion at low temperatures through a combination of: (i) high mixing intensities (i.e. facilitating high rates of mass transfer); and (ii) enhanced retention of psychroactive biomass (Lettinga *et al*., 2001; Alvarado-Lassman *et al*., 2008; McKeown *et al*., 2012). However, failure of the bioreactors to retain granular sludge during LTAD may lead to severe hydraulic washout of psychro-active sludge (Lettinga *et al*., 1999). Therefore, non-granule-based systems using inert nuclei to promote re-granulation could be of advantage during psychrophilic reactor operation (McKeown *et al*., 2009b).

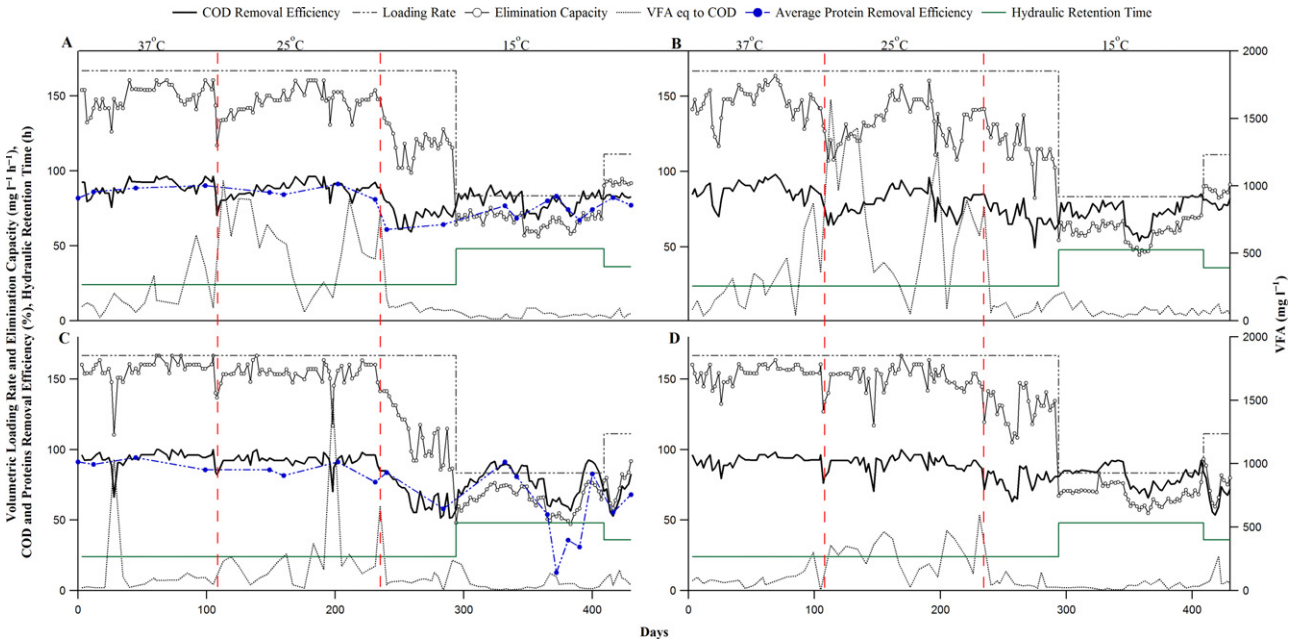

Fig. 1. Process performance of the inverted fluidized bed (IFB): (A) IFB2 and (B) IFB1; and expanded granular sludge bed (EGSB): (C) EGSB2 and (D) EGSB1 reactors.

Knowledge gaps remain, however, regarding the nature and function of the microbial populations involved in LTAD, which are a deterrent to full-scale applications (McKeown *et al.*, 2009b; 2012). This information deficit is mainly due to the complex relationship between wastewater characteristics, process conditions and dynamics in microbial community structure. In an attempt to link microbial functional groups with process performance, we studied community dynamics in two different methanogenic anaerobic reactor configurations [i.e. an inverted fluidized bed (IFB) containing fixed fluidized biomass on the support particles and an expanded granular sludge bed (EGSB) containing crushed granular biomass], during operational temperature transitions from 37°C to 25°C, and from 25°C to 15°C. The present study is a continuation of the experiment described in Bialek and colleagues (2011), therefore a similar experimental approach has been employed. The methanogenic community structure and dynamics were examined qualitatively by DGGE and quantitatively by real-time PCR, the results were then statistically analysed and compared. We hypothesized that the process performance and microbial community structure and dynamics can be influenced by the reactor configuration during transition from mesophilic to psychrophilic reactor operation and by changes applied to the loading rate and hydraulic retention time (HRT).

Results

Process performance

The process efficiency depended on the operational temperature (Fig. 1): during operation at 37°C (period I) and 25°C (period II), the replicated IFB and EGSB reactors exhibited a similar level of performance exceeding 80% COD removal efficiency (RE) and elimination capacity (EC) of 139 ± 13 and 148 ± 8 mg COD l^{-1} h^{-1} for IFB1 and IFB2; and EC of 152 ± 8 and 155 ± 8 mg COD l^{-1} h^{-1} for EGSB1 and EGSB2) and > 80% protein removal efficiency (PRE; Fig. 1); with > 60% methane content in the biogas (data not shown). The effluent concentrations of volatile fatty acids (VFA) fluctuated, with maximum values of > 1500 mg COD l^{-1} in the IFB and EGSB reactors.

The decrease in operational temperature to 15°C resulted in a gradual reduction in the treatment efficiency, an instantaneous decrease in residual VFA concentrations (< 200 mg COD l^{-1}) and a significant drop in PRE, to 60% (Fig. 1). The IFB reactors, however, recovered after the temperature decrease and recorded stable > 70% COD RE within 30 days (Fig. 1). The EGSB reactors displayed a greater initial decline in performance (EGSB1 to 60% COD RE, EC of 105 mg COD l^{-1} h^{-1} and EGSB2 to 50% COD RE, EC of 86 mg COD l^{-1} h^{-1}), although EGSB1 returned to a more stable COD RE afterwards (Fig. 1).

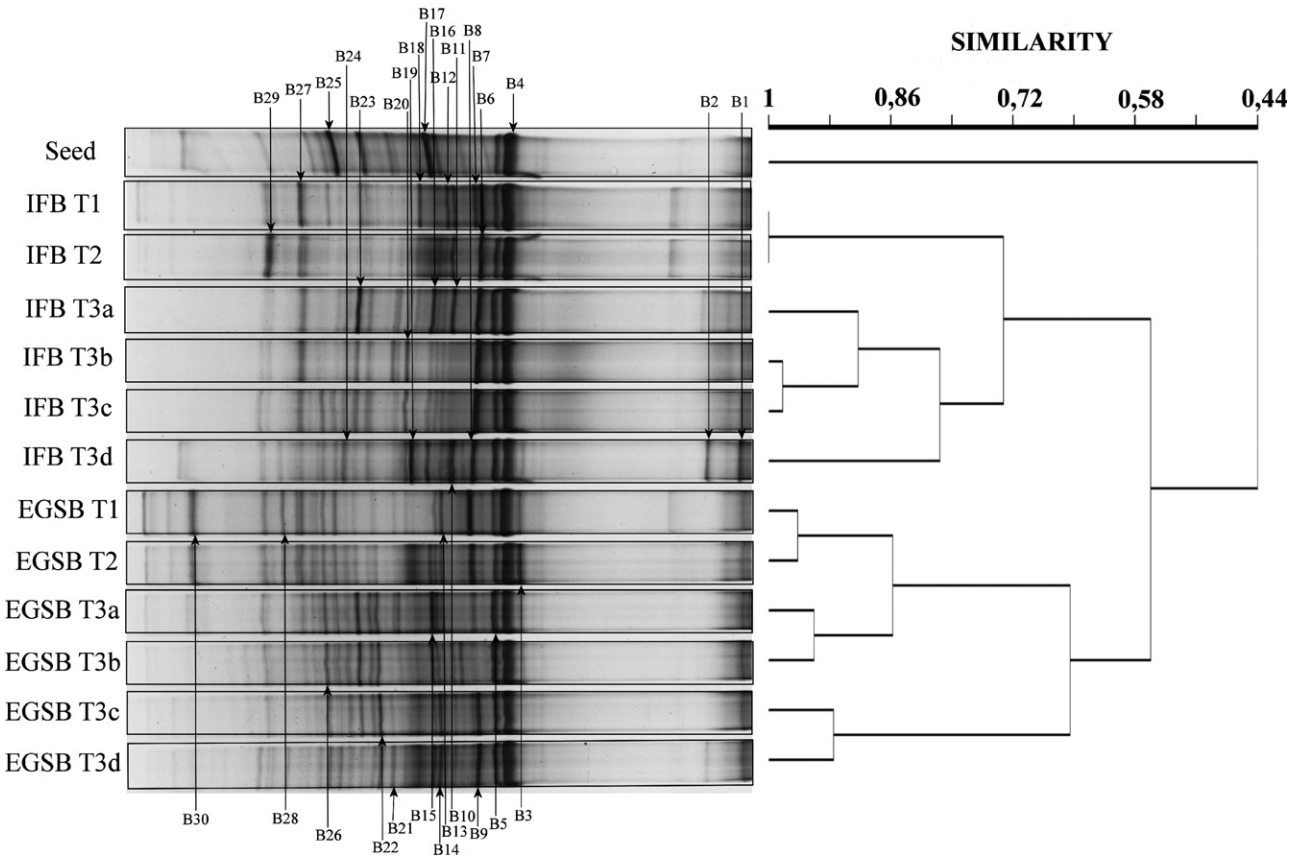

Fig. 2. Unweighted pair group method with arithmetic mean (UPGMA) cluster analysis of the 16S rRNA gene fragments generated from bacterial denaturing gradient gel electrophoresis (DGGE) profiles of IFB2 and EGSB2 biomass. Similarity calculated by Sørensons (Bray–Curtis) distance measurement. B1–B30 indicates bands used for sequencing and phylogenetic analyses.

The applied HRT was increased to 48 h on day 294, resulting in an increase in the treatment efficiency of all four reactors (Fig. 1). An unexpected temperature decrease (to 6°C), due to a heating pump failure on day 350, destabilized all systems but a more pronounced deterioration in the PRE (13% PRE) was observed in the EGSB system (Fig. 1). After recovery and stabilization, where the COD RE of all four reactors exceeded 80%, the applied HRT to both systems was reduced to 36 h, on day 409. Interestingly, the performance of the IFB reactors remained very stable with > 78% COD RE and > 77% PRE (Fig. 1), while a significant transient drop in the treatment efficiency of the EGSB reactors occurred (to 50% COD RE and 55% PRE; Fig. 1).

Bacterial DGGE and UPGMA cluster analysis

Comparative polymerase chain reaction-denaturing gradient gel electrophoresis (PCR-DGGE) analysis of the bacterial populations in the reactors identified configuration-dependent differences. Unweighted pair group method with arithmetic mean (UPGMA) cluster analysis revealed that the composition and development of the bacterial portion of the microbial communities in the IFB and EGSB reactors was distinctively different (e.g. < 58% similarity between IFB2 and EGSB2; Fig. 2) during the trial. Identical DGGE profiles (100% similarity) were recorded from the IFB reactor at 37°C (IFB T1) and 25°C (IFB T2). The profiles changed, however, following the temperature reduction to 15°C (IFB T3abcd; 72% similarity). Likewise, similar communities (> 95% similarity) at 37°C (EGSB T1) and 25°C (EGSB T2) within the EGSB reactor changed immediately after temperature reduction to 15°C (EGSB T3ab; 86% similarity). Furthermore, subsequent changes in the EGSB bacterial populations (EGSB T3cd) resulted in < 72% similarity to the former profiles (Fig. 2).

Bacterial and archaeal phylogenetic analysis

In total, 30 DGGE bands, designated as B1–B30, were retrieved from the bacterial DGGE gel and used for subsequent sequencing analysis. Ten bands out of the 30 (B1, B2, B7, B10, B11, B16, B18, B19, B20, B24) were unique to the IFB reactor and 15 common bands were noted between the IFB and EGSB reactors (Table 1;

Table 1. Phylogenetic affiliation of the 16S rRNA gene sequences from bacterial DGGE bands B1–B30 (accession numbers: JF927800–JF927829).

Band number	Nearest species and taxon	Phylogenetic affiliation to phylum	Similarity (%)	Accession No.	Reactor biomasses containing the respective bands
B1 JF927800	*Rikenellaceae* bacterium	*Bacteroidetes*	99	AB298736	IFB T3d (day 430)
B2 JF927801	*Rikenellaceae* bacterium	*Bacteroidetes*	100	AB298736	IFB T3d (day 430)
B3 JF927802	Uncultured *Bacteroides* sp.	*Bacteroidetes*	100	EU214534	EGSB T1 T2 T3ab (days 106, 195, 298, 365)
B4 JF927803	Uncultured *Deltaproteobacteria*	*Proteobacteria*	99	CU918377	Seed; IFB&EGSB T1 T2 T3 abcd (days 106, 195, 298, 365, 409, 430)
B5 JF927804	*Bacillus macyae*	*Firmicutes*	98	NR025650	Seed; IFB&EGSB T1 T2 T3 abcd (days 106, 195, 298, 365, 409, 430)
	Bacillus alkalidiazotrophicus	*Firmicutes*	98	NR044420	
	Anaerobacillus alkalilacustre	*Firmicutes*	98	DQ675454	
B6 JF927805	Uncultured anaerobic bacterium	*Bacteroidetes*	99	AY953210	IFB&EGSB T1 T2 T3 abcd (days 106, 195, 298, 365, 409, 430)
B7 JF927806	Uncultured *Bacteroidetes* bacterium	*Bacteroidetes*	99	JN998178	IFB T1 (day 106)
B8 JF927807	Uncultured anaerobic bacterium	*Bacteroidetes*	99	AY953210	IFB&EGSB T1 T2 T3 abcd (days 106, 195, 298, 365, 409, 430)
B9 JF927808	Uncultured anaerobic bacterium	*Bacteroidetes*	99	AY953210	IFB&EGSB T1 T2 T3 abcd (days 106, 195, 298, 365, 409, 430)
B10 JF927809	*Fusibacter* sp.	*Firmicutes*	96	AF491333	IFB T3d (day 430)
	Fusibacter paucivorans	*Firmicutes*	95	NR024886	
B11 JF927810	*Porphyromonadaceae* bacterium	*Bacteroidetes*	99	GU247220	IFB T1 T2 T3a (days 106, 195, 298)
	Parabacteroides sp.	*Bacteroidetes*	98	JN029805	
B12 JF927811	*Bacteroidetes* bacterium	*Bacteroidetes*	99	AB623230	IFB&EGSB T1 T2 T3 abcd (days 106, 195, 298, 365, 409, 430)
B13 JF927812	Uncultured *Bacteroidetes* bacterium	*Bacteroidetes*	100	CU926896	IFB&EGSB T1 T2 T3 abcd (days 106, 195, 298, 365, 409, 430)
B14 JF927813	Uncultured anaerobic bacterium	*Bacteroidetes*	99	AY953210	IFB&EGSB T1 T2 T3 abcd (days 106, 195, 298, 365, 409, 430)
B15 JF927814	*Clostridium* sp.	*Firmicutes*	97	HQ326746	EGSB T2 T3 abcd (days 195, 298, 365, 409, 430)
	Clostridium lactatifermentans	*Firmicutes*	97	NR025651	
B16 JF927815	*Parabacteroides* sp.	*Bacteroidetes*	99	JN029805	IFB T3 abcd (days 298, 365, 409, 430)
	Porphyromonadaceae bacterium	*Bacteroidetes*	99	GU247220	
B17 JF927816	*Pseudomonas* sp.	*Proteobacteria*	99	HM468091	Seed
B18 JF927817	*Bacteroidetes* bacterium	*Bacteroidetes*	99	AB623230	IFB T1 T2 T3 a (days 106, 195, 298)
B19 JF927818	*Fusibacter* sp.	*Firmicutes*	96	AF491333	IFB T3 bcd (days 365, 409, 430)
	Fusibacter paucivorans	*Firmicutes*	96	NR024886	
B20 JF927819	*Clostridiaceae* bacterium	*Firmicutes*	98	AB298771	IFB T1 T2 T3 abcd (days 106, 195, 298, 365, 409, 430)
	Clostridium aminobutyricum	*Firmicutes*	98	X76161	
B21 JF927820	*Acetobacterium carbinolicum*	*Firmicutes*	99	AB546239	IFB&EGSB T3 abcd (days 298, 365, 409, 430)
	Acetobacterium psammolithicum	*Firmicutes*	99	AF132739	
B22 JF927821	Uncultured *Clostridium*	*Firmicutes*	97	GQ390389	EGSB T2 T3 abcd (days 195, 298, 365, 409, 430)
B23 JF927822	*Proteocatella sphenisci*	*Firmicutes*	99	NR041885	IFB&EGSB T1 T2 T3 abcd (days 106, 195, 298, 365, 409, 430)
B24 JF927823	Uncultured *Firmicutes*	*Firmicutes*	100	CU926541	IFB T3 abcd (Day 298, 365, 409, 430)
B25 JF927824	*Syntrophobacter pfennigii*	*Proteobacteria*	95	NR026232	Seed; IFB&EGSB T1 T2 T3 abcd (days 106, 195, 298, 365, 409, 430)
	Syntrophobacteraceae bacterium	*Proteobacteria*	94	FJ040958	
	Syntrophobacter wolinii	*Proteobacteria*	94	NR028020	
B26 JF927825	Uncultured *Pelospora*	*Firmicutes*	100	HQ183799	Seed; IFB T1 T2 T3 cd (days 106, 195, 409,430); EGSB T1 T2 T3 abcd (days 106, 195, 298, 365, 409, 430)
B27 JF927826	*Atopobium* sp.	*Actinobacteria*	95	HQ616400	IFB&EGSB T1 T2 T3 abcd (days 106, 195, 298, 365, 409, 430)
B28 JF927827	*Syntrophobacter sulfatireducens*	*Proteobacteria*	100	NR043073	IFB&EGSB T1 T2 T3 d (days 106, 195,430)
B29 JF927828	*Syntrophomonas wolfei*	*Firmicutes*	97	DQ666176	Seed; IFB&EGSB T1 T2 T3 abcd (days 106, 195, 298, 365, 409, 430)
B30 JF927829	Uncultured *Geobacter*	*Proteobacteria*	99	EF658630	EGSB T1 T2 (days 106, 195)

Fig. 3A). In the archaeal DGGE gel, a total of 9 bands (A1–A9) were retrieved and sequenced (Table 2; Fig. 3B).

Dynamic changes in archaeal populations observed by real-time PCR

The EGSB and IFB reactors displayed a noticeable disparity in terms of the quantitative composition of the archaeal populations within the methanogenic community during the trial (Fig. 4A and B). In particular, a notable difference between the samples taken during mesophilic (37°C to 25°C) and psychrophilic (15°C) reactor operation was an increase in the relative abundance and absolute quantity of the hydrogenotrophic order *Methanomicrobiales* (MMB), which became by far the most prominent group in all reactors under low-temperature conditions. During mesophilic operation, MMB accounted for only 2.5–3.6% ($2.9–4.3 \times 10^5$ copies ml^{-1}) of the total methanogenic 16S rRNA gene concentration in IFB2 and IFB1 and 0.0–3.3% (1.4×10^4 to 1.1×10^6 copies ml^{-1}) in EGSB2 and EGSB1 respectively. The emergence to predominance of MMB was evident in all reactors. In IFB1 and IFB2, the relative abundance of this group had reached 52.8% (1.5×10^7 copies ml^{-1}) and 96.7% (4.7×10^8 copies ml^{-1}) of the total methanogenic 16S rRNA gene concentration by the end of the trial. In EGSB2 and EGSB1 MMB accounted for respectively 45.7% (3.1×10^7 copies ml^{-1}) and 87.7% (1.2×10^8 copies ml^{-1}) of the total methanogenic 16S rRNA gene concentration by day 430.

The aceticlastic family *Methanosaetaceae* (Mst) was the most abundant group in the seed biomass accounting for 58.4% of the total methanogenic 16S rRNA gene concentration. During 37°C reactor operation, the 16S rRNA gene concentration of Mst was detected at 2.1×10^6 and 3.1×10^6 copies ml^{-1} (18.0% and 26.2% of the total methanogenic 16S rRNA gene concentration) in the IFB2 and IFB1 respectively. In EGSB2 and EGSB1, the 16S rRNA gene concentration of Mst was 5.0×10^6 and 1.5×10^7 copies ml^{-1} (16.1% and 42.9% of the total methanogenic 16S rRNA gene concentration) respectively. At the end of the trial at 15°C, an increase in the 16S rRNA gene concentration of this group was detected at 9.9×10^6 and 1.1×10^7 copies ml^{-1} (2.0% and 38.9% of the total methanogenic 16S rRNA gene concentration) in IFB2 and IFB1 respectively. A similar trend was observed in EGSB1 and EGSB2 with the 16S rRNA gene concentration of $1.5–3.0 \times 10^7$ copies ml^{-1} (10.6–45.0% of the total methanogenic 16S rRNA gene concentration).

The aceticlastic family, *Methanosarcinaceae* (Msc), was only detected (i.e. $> 1.28 \times 10^1$ copies μl^{-1}) in the IFB reactors, and this could have been influenced by the presence of this group during previous experiment as described in Bialek and colleagues (2011), since the present experiment is a continuation of this former work. The 16S rRNA gene concentration of this group showed a marked increase from 1.6×10^4 and 6.5×10^3 (0.1% and 0.1% of the total methanogenic 16S rRNA gene concentration) at 37°C to 5.3×10^5 and 2.6×10^6 copies ml^{-1} (1.8 and 0.5% of the total methanogenic 16S rRNA gene concentration) at 15°C in, respectively, IFB1 and IFB2. *Methanosarcina* numbers could have increased and remained above the detection limit (presumably by retention in biofilms during mesophilic operation with high accumulation of VFA) when the IFB reactors were later operated at 15°C, although no accumulation of acetic acid (reported to be associated with the appearance of *Methanosarcina* and process deterioration (O'Reilly *et al*., 2009) was observed during that period (period III; Fig. 1).

The hydrogenotrophic order *Methanobacteriales* (MBT) was the most dominant group at mesophilic temperatures and the 16S rRNA gene concentration of this group was detected at $8.3–9.3 \times 10^6$ copies ml^{-1} (70.1–79.4% of the total methanogenic 16S rRNA gene concentration) in IFB1 and IFB2, and $1.8–2.6 \times 10^7$ copies ml^{-1} (53.8–83.9% of the total methanogenic 16S rRNA gene concentration) in EGSB1 and EGSB2. Following a reduction in the temperature to 15°C, a decrease in the 16S rRNA gene concentration of this group was observed at $1.9–3.4 \times 10^6$ copies ml^{-1} (6.2 to 0.7% of the total methanogenic 16S rRNA gene concentration) in IFB1 and IFB2, and $2.4–6.4 \times 10^6$ copies ml^{-1} (1.7–9.4% of the total methanogenic 16S rRNA gene concentration) in EGSB1 and EGSB2.

Quantitative shifts in archaeal populations

Quantitative shifts in the methanogenic communities were visualized using the non-metric multidimensional scaling (NMS) technique and moving-window analysis, based on real-time PCR data. Unlike presented by Bialek and colleagues (2011), the absolute quantity-matrix based on 16S rRNA gene concentration data appeared to be more applicable in describing the transition from mesophilic to psychrophilic temperature operation with community shift towards hydrogenotrophic methanogens during the 430-day trial (Fig. 5A and B).

In the NMS plot, the cumulative r^2 represented by the axes was > 0.9, the final stress value was < 5, and instability was $< 10^{-4}$ (Fig. 5A). This indicates that our results meet the criteria for an excellent representation (McCune and Grace, 2002). The NMS results revealed that the archaeal populations in the reactors shifted in a different manner and grouped separately in response to decreasing temperature (Fig. 5A), despite the identical operating conditions. This suggests that the reactor configuration may have a significant effect on the shaping of the methanogenic community structure. The absolute quantity

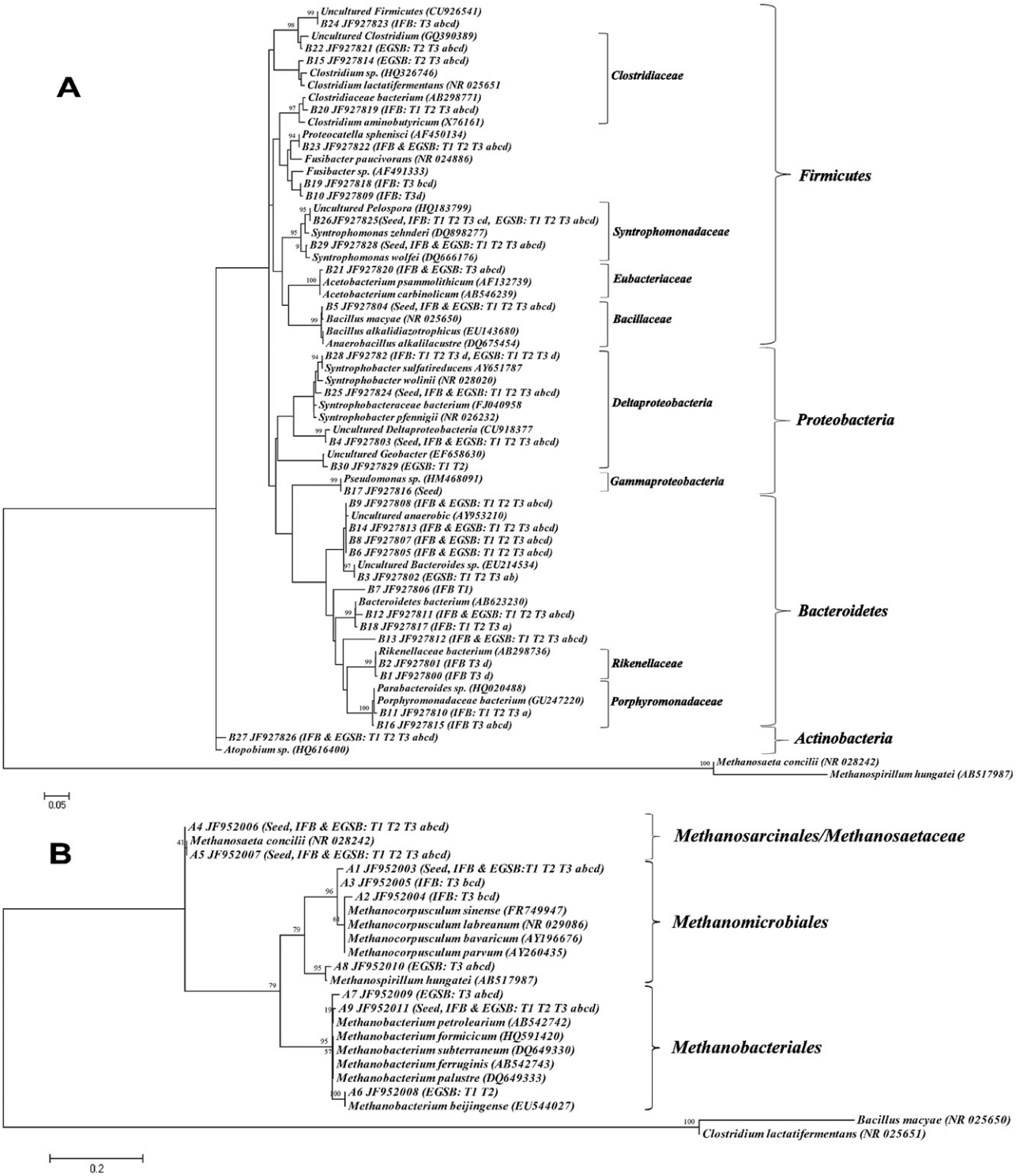

Fig. 3. Neighbour-joining tree illustrating the phylogenetic affiliations of the 16S rRNA gene sequences obtained from: (A) bacterial DGGE bands B1–B30 (accession numbers: JF927800–JF927829) and (B) archaeal DGGE bands A1–A9 (accession numbers: JF952003–JF952011). Reactor biomasses containing the respective bands are given in parenthesis.

Table 2. Phylogenetic affiliation of the 16S rRNA gene sequences from archaeal DGGE bands A1–A9 (accession numbers: JF952003–JF952011).

Band number	Nearest species and taxon	Phylogenetic affiliation to order	Similarity (%)	Accession No.	Reactor biomasses containing the respective bands
A1 JF952003	*Methanocorpusculum sinense*	*Methanomicrobiales*	99	FR749947	Seed; IFB&EGSB T1 T2 T3 abcd (days 106, 195, 298, 365, 409, 430)
	Methanocorpusculum labreanum		99	NR029086	
	Methanocorpusculum bavaricum		99	AY196676	
	Methanocorpusculum parvum		99	AY26043	
A2 JF952004	*Methanocorpusculum sinense*	*Methanomicrobiales*	99	FR749947	IFB T3 bcd (days 365, 409, 430)
	Methanocorpusculum labreanum		99	NR029086	
	Methanocorpusculum bavaricum		99	AY196676	
	Methanocorpusculum parvum		99	AY26043	
A3 JF952005	*Methanocorpusculum sinense*	*Methanomicrobiales*	99	FR749947	IFB T3 bcd (days 365, 409, 430)
	Methanocorpusculum labreanum		99	NR029086	
	Methanocorpusculum bavaricum		99	AY196676	
	Methanocorpusculum parvum		99	AY26043	
A4 JF952006	*Methanosaeta concilii*	*Methanosarcinales*	99	NR028242	Seed; IFB&EGSB T1 T2 T3 abcd (days 106, 195, 298, 365, 409, 430)
A5 JF952007	*Methanosaeta concilii*	*Methanosarcinales*	100	NR028243	Seed; IFB&EGSB T1 T2 T3 abcd (days 106, 195, 298, 365, 409, 430)
A6 JF952008	*Methanobacterium beijingense*	*Methanobacteriales*	99	EU544027	EGSB T1 T2 (days 106, 195)
A7 JF952009	*Methanobacterium petrolearium*	*Methanobacteriales*	99	AB542742	EGSB T3 abcd (days 298, 365, 409, 430)
	Methanobacterium formicicum		98	HQ591420	
	Methanobacterium ferruginis		98	AB542743	
	Methanobacterium subterraneum		98	DQ649330	
	Methanobacterium palustre		98	DQ649333	
A8 JF952010	*Methanospirillum hungatei*	*Methanomicrobiales*	99	AB517987	EGSB T3 abcd (das 298, 365, 409, 430)
A9 JF952011	*Methanobacterium petrolearium*	*Methanobacteriales*	99	AB542742	Seed; IFB&EGSB T1 T2 T3 abcd (days 106, 195, 298, 365, 409, 430)
	Methanobacterium formicicum		99	HQ591420	
	Methanobacterium ferruginis		99	AB542743	
	Methanobacterium subterraneum		99	DQ649330	
	Methanobacterium palustre		99	DQ649333	

matrix clearly demonstrated a remarkable shift in community structure of the IFB reactors when lowering the temperature (IFB1–I1 and IFB2–I2 from T2 – 25°C to T3a – 15°C). Wide shifts, which were especially prominent after transition to 15°C (IFB1–I1 and IFB2–I2 from T3a to T3d), were paralleled by the rapid increase in MMB and Msc populations during the corresponding period. Interestingly, the EGSB matrices showed much smaller shifts in community structure following temperature decrease (EGSB1–E1 and EGSB2–E2 from T2 – 25°C to T3a – 15°C). Subsequently, at 15°C a similar trend as in the IFB reactors was observed in the community shift of the EGSB reactors, although much slower than in the IFB reactors. This shift can be mostly attributed to increasing MMB and Mst populations (EGSB1–E1 and EGSB2–E2 from T3a to T3d). Consequently, the IFB and EGSB matrices were located distantly based on samples taken during 15°C operation, demonstrating the different community composition of IFB and EGSB reactors, which could be attributed to slower adaptation of the EGSB biomass to the lower temperature (Fig. 5A).

Moving-window analysis was applied to observe dynamic shifts in the community composition of the IFB and EGSB reactors (Fig. 5B). An approach based on the absolute quantity of target methanogenic groups was employed to visualize shifts in quantitative community composition. Moving-window output of the IFB reactors showed a significant dissimilarity of 87–88% in the IFB1 and IFB2 between T2 (day 195) and T3a (day 298), and between T3a (day 298) and T3b (day 365). In contrast, the output from the EGSB reactors indicated 56–51% dissimilarity in the EGSB1 and EGSB2 between T3b (day 365) and T3c (day 409), and between T3c (day 409) and T3d (day 430). The time difference in shifts of the methanogenic communities between the IFB and EGSB reactors could indicate that the IFB reactors responded much quicker to the temperature decrease to 15°C, while in the EGSB reactors this change was slower and methanogenic communities required more time to adapt (Fig. 5B).

Discussion

Process performance

Dairy wastewater is a complex substrate composed of easily degradable carbohydrates, mainly lactose, and less bioavailable proteins and lipids (Fang and Yu, 2000;

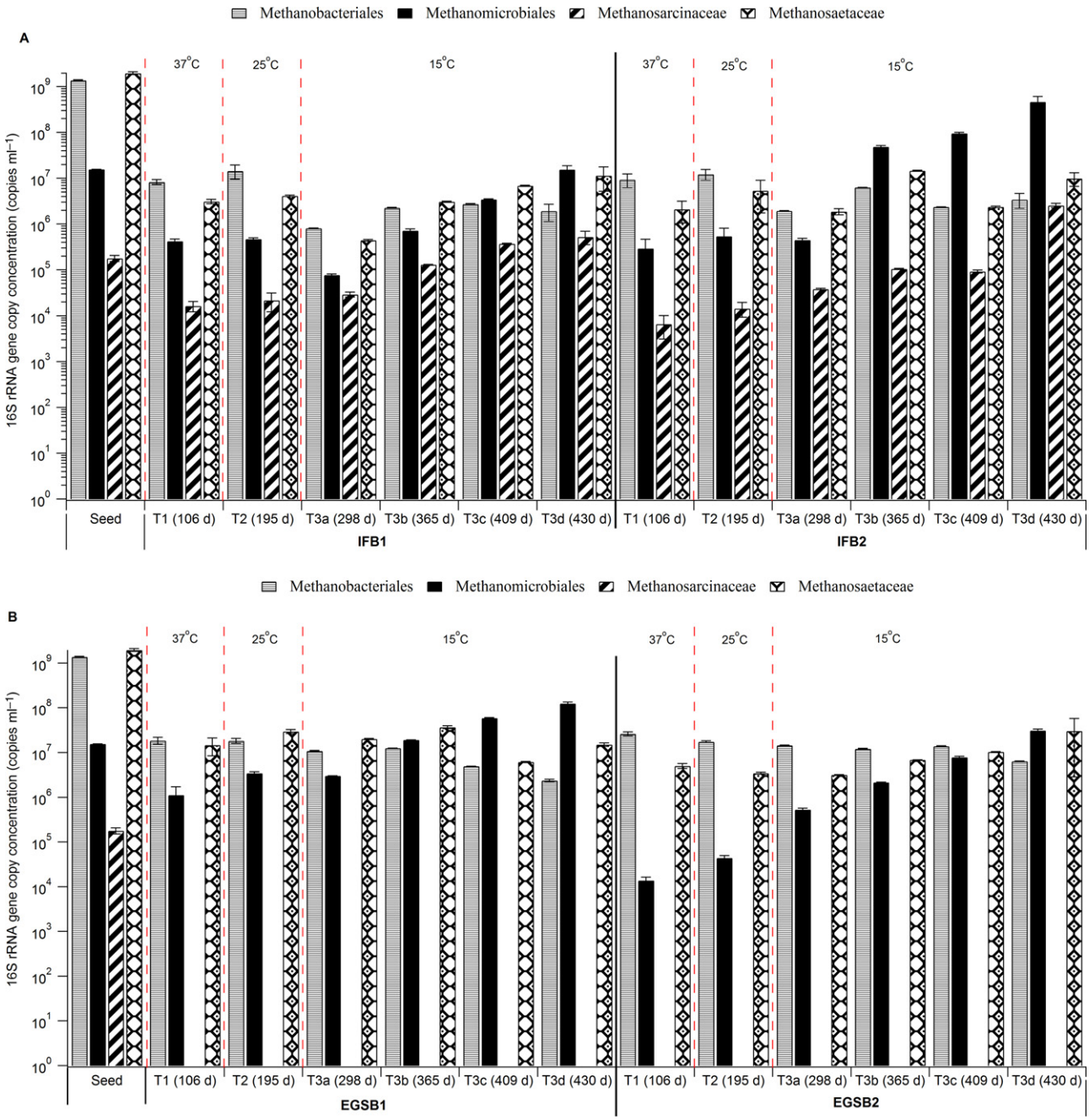

Fig. 4. Absolute quantification of the 16S rRNA gene concentration of the methanogenic/archaeal populations during transition from mesophilic (37°C to 25°C) to psychrophilic (15°C) reactor operation in the (A) IFB and (B) EGSB reactors.

Tommaso *et al.*, 2003). The latter are responsible for the typical problems associated with high-rate AD of dairy waste effluents (Perle *et al.*, 1995). Hydrolysis of proteins and lipids is reported to strongly decline with decreasing temperature, especially approaching 15°C (Tommaso *et al.*, 2003). Given these reports, and considering the fact that skimmed dairy wastewater was used in the present study (Table 3), decreased protein degradation/hydrolysis

Table 3. Composition of skimmed-milk powder.

Parameter	% of COD	COD (mg l^{-1})
Proteins	40	1600
Sugars	55	2200
Fats	1	40
Others	4	160
Total	100	4000

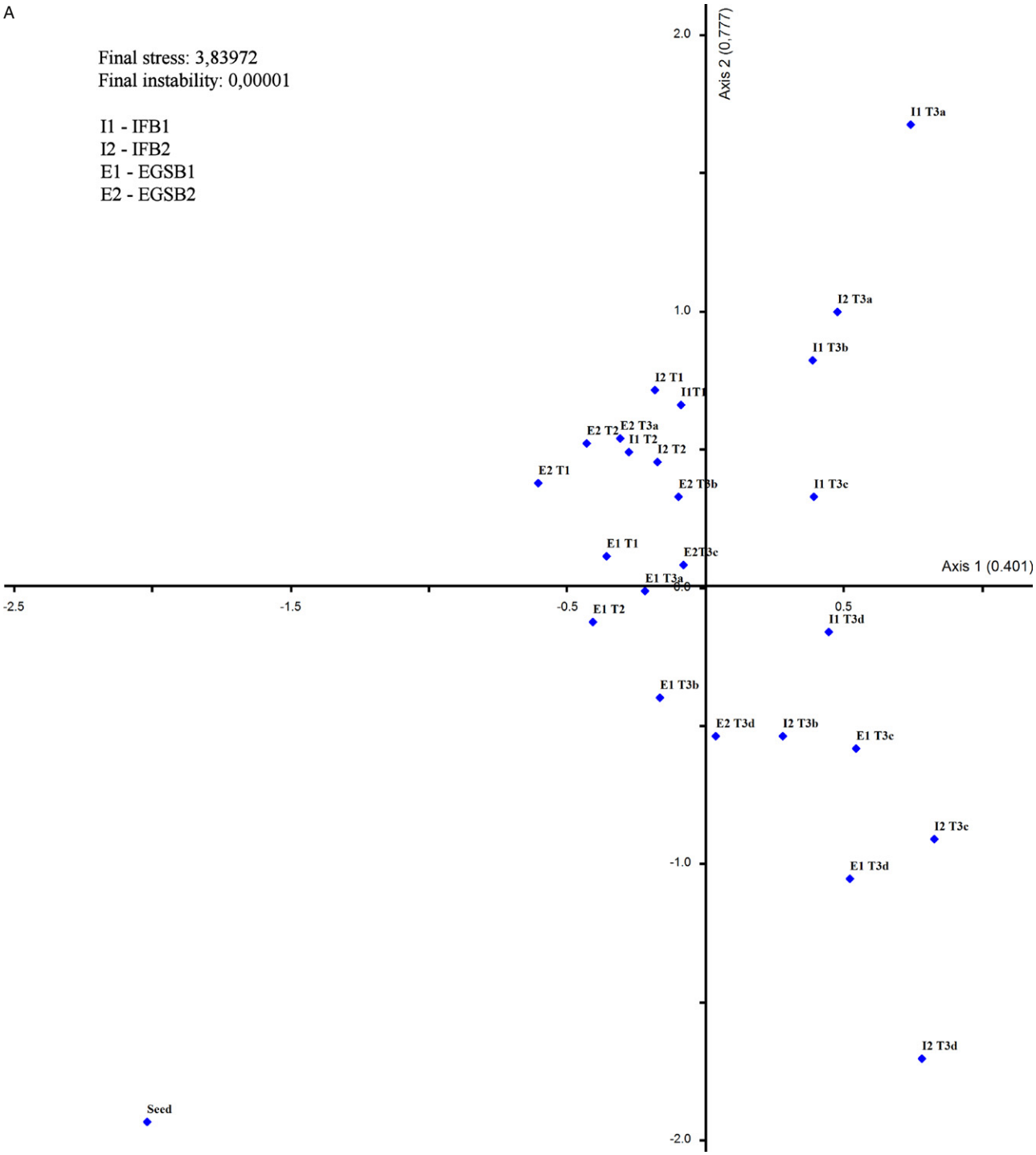

Fig. 5. Quantitative shifts in archaeal populations analysed based on the absolute quantity of target methanogenic groups present in the IFB and EGSB reactors and measured by real-time PCR by (A) non-metric multidimensional scaling (NMS) and (B) moving-window analysis. T1 (37°C, day 106); T2 (25°C, day 195); T3a (15°C, day 298), T3b (15°C, day 365); T3c (15°C, day 409), T3d (15°C, day 430).

can be assumed to be mainly responsible for the declining process performance in our digesters.

Casein is the major protein in milk (up to 80% of the total proteins) and in dairy effluents. When fed to acclimated anaerobic reactors, degradation of casein is rapid, due to strong proteolytic activity, and the degradation products are non-inhibitory (Perle *et al.*, 1995). This was likely the case in the systems investigated, with > 80% PRE recorded during acclimated mesophilic conditions of 37–25°C (Fig. 1). The fluctuations in effluent VFA con-

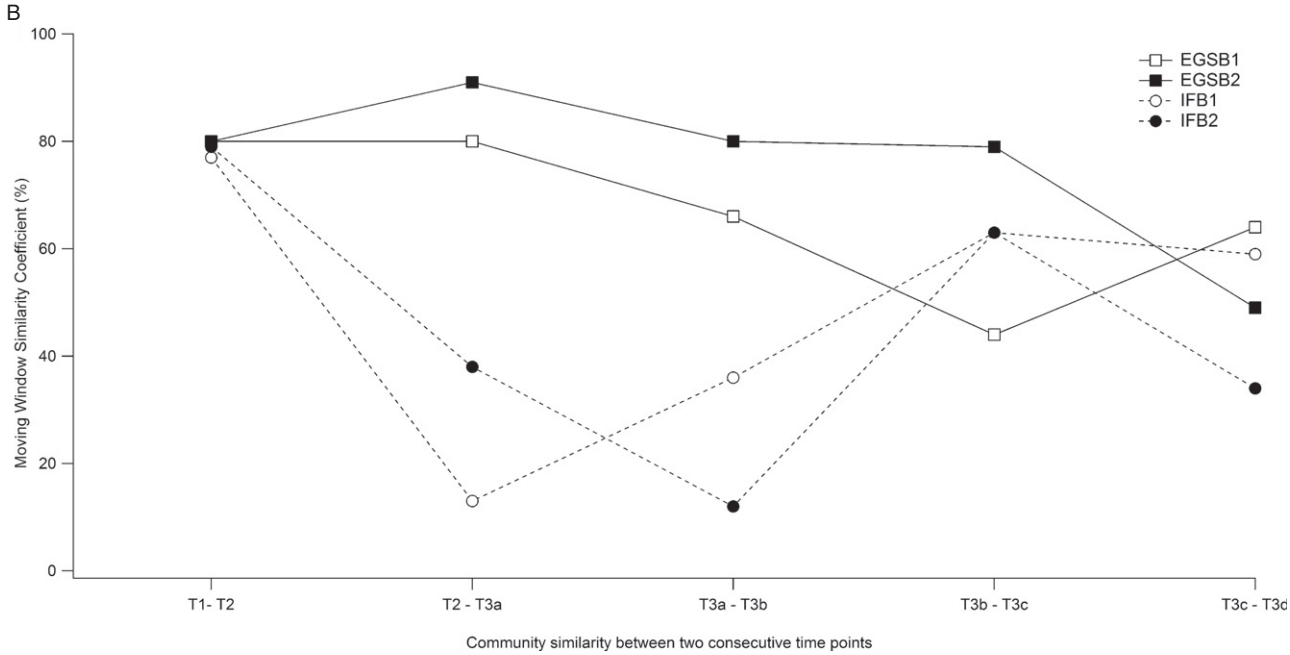

Fig. 5. *Cont.*

centration (Fig. 1) observed at mesophilic temperatures were therefore, most probably due to rapid hydrolysis and fermentation of carbohydrates and proteins into VFA. A gradual decrease in COD RE (Fig. 1), however, occurred immediately after the temperature reduction to 15°C, coupled with an instantaneous decrease in residual VFA concentrations and significant drop in PRE of *c*. 60% in the IFB and EGSB reactors. Since no VFA build-up was observed at 15°C, it is considered that protein hydrolysis had become the rate-limiting step.

Following the immediate drop in PRE to 60%, the IFB system demonstrated a successful adaptation to low temperature operation and, after a brief temporal instability, > 78% COD RE and > 77% PRE was recorded at psychrophilic, steady-state operation (Fig. 1). On the other hand, the EGSB system displayed a slower adaptation to low temperature operation, with a performance of 58% PRE 45 days after the temperature decrease, and long unstable performance, with minimum values of 13% PRE and < 60% COD RE (Fig. 1).

We propose that the better flexibility and adaptability of the IFB biomass to low temperature might originate from the spatial arrangement of fixed fluidized biomass that developed in the IFB (Fig. S1) playing an important role in differences in transfer of intermediates and optimal degradation of substrates (Grotenhuis *et al*., 1991). At low temperatures, the viscosity of effluents increases and, therefore, the diffusion of soluble compounds will drop, particularly in sludge bed reactors that become less easily mixed (Lettinga *et al*., 2001). There was no evidence of granulation of the biomass in the EGSB reactor, which was seeded with crushed granular sludge as inoculum and the biomass remained a non-granular floculant sludge throughout the trial (Fig. S1). Furthermore, the advantage of the IFB configuration over the EGSB in this experiment might arise from the use of floatable particles with a specific density lower than the liquid, thus particles were fluidized downward (Garcia-Calderon *et al*., 1998) and better substrate–biomass contact might be attained. Due to the large specific area, the support particles can retain more biomass (Alvarado-Lassman *et al*., 2008), which is especially crucial during transitional and permanent changes in operating conditions, like the temperature variation investigated in this study.

Microbial population dynamics

Understanding the impact of disturbances, such as temperature shocks or permanent temperature decrease, on process stability and performance will undoubtedly shed more light on the process of LTAD when placed in the context of microbial community dynamics. Together with increased knowledge on the impact of reactor configuration on the functional stability of microbial communities, informed decisions can be enabled regarding the optimal reactor type and process conditions for a given wastewater. A robust LTAD system must possess the ability to maintain process stability in response to disturbances and it has been reported that in general systems with more dynamic communities have greater functional and process stability (Hashsham *et al*., 2000; Carballa *et al*., 2011; Werner *et al*., 2011). We thus considered our data in

the context of the model proposed by Allison and Martiny (2008), which divides the population dynamics that maintain community function over time into three basic mechanisms (resistance, resilience or redundancy) to address the process performance of the IFB and EGSB reactors investigated.

A microbial community is resistant if it is similar across a variety of environmental conditions and, therefore, it is difficult to perturb from an original state (Allison and Martiny, 2008). Initially, identical bacterial populations at mesophilic temperatures, as observed by the UPGMA cluster analysis, suggested resistance of the bacterial populations composition (Fig. 2): 100% similarity between IFB T1 (37°C) and IFB T2 (25°C) and > 95% similarity between EGSB T1 (37°C) and EGSB T2 (25°C). A similar trend was observed with the archaeal population behaviour between the two studied mesophilic temperatures where, for example, the EGSB and the IFB populations showed 80% similarity between T1 (37°C) and T2 (25°C) based on the NMS and moving window matrix (Fig. 5A and B). The methanogenic community composition was thus resistant to the temperature change from 37°C to 25°C, indicating metabolic flexibility and physiological tolerance to the applied disturbance in this mesophilic temperature range. A further temperature decrease to 15°C showed that the community was, however, sensitive to the disturbance and resulted in an altered microbial composition (Fig. 5A and B), indicating that the community responded to the second temperature disturbance using one of the mechanisms discussed below.

The microbial composition of reactor biomass is resilient if it is sensitive to a disturbance and changes, but quickly recovers to its initial composition (Allison and Martiny, 2008). This mechanism was not observed in the systems and timescale investigated because after the disturbance the community did not return to its original composition. Werner and colleagues (2011) reported that resilience was important to maintain the function of syntrophic populations over time in mesophilic brewery wastewater treatment facilities. These authors concluded that syntrophic bacteria had very specialized metabolic functions within the overall trophic structure, which made them more likely to rebound after a disturbance, rather than undergoing competitive growth with different syntrophs that have a similar function in the microbial consortium.

Whether the microbial composition rebounds, or not, is possibly determined by the severity of the disturbance and importance of the disturbance on the process stability and performance. It may be possible, for example, that the microbial composition of the anaerobic reactor subjected to a slight variation or short disturbance in environmental conditions returns to its original composition after such a disturbance. Madden and colleagues (2010) investigated the effect of transient (but severe) perturbations on the methanogenic community structure and process performance of replicate EGSB-based reactors. Their cluster analyses of DGGE data suggested that temporal shifts in microbial community structure were predominantly independent of the applied perturbations (Madden *et al.*, 2010), although it is important to point out that community dynamics were monitored only via DGGE, where gel-to-gel variation and relatively low sensitivity (compared with qPCR) are limiting to ensure reproducibility and detection of minor populations or subtle population changes (Talbot *et al.*, 2008). Recent studies point out the limitations of studies based only on the DNA (Raes and Bork, 2008; Nelson *et al.*, 2011; Wendeberg *et al.*, 2012). Future studies should therefore focus on functional investigations to unravel metabolic activity of the microbial communities underpinning the AD processes.

When the community composition is sensitive, and not resilient, it might produce process rates similar to the original community in case the members of the community are functionally redundant (Allison and Martiny, 2008). The highly dynamic community structure during well-functioning periods (Fig. 5A and B) may be explained by the functional redundancy among diverse phylogenetic groups, allowing oscillations of their populations, due to the presence of a reservoir of species able to perform the same ecological function with no effects on the reactor performance (Zumstein *et al.*, 2000; Briones and Raskin, 2003). The stability of reactor performance, especially that of the IFB reactors, after the temperature shift from 25°C to 15°C and consequent change in methanogenic community composition, could be explained by functional redundancy in one, or more, steps of the methanogenic pathway.

Microbial community composition

Methanogenesis can proceed through two pathways, where acetate and/or hydrogen and carbon dioxide are converted into methane, termed as aceticlastic methanogenesis and hydrogenotrophic methanogenesis respectively. Under certain conditions, homoacetogenic bacteria can compete with hydrogenotrophic methanogenesis for hydrogen (hydrogen is used to reduce carbon dioxide to acetate (Lovley and Klug, 1983). Homoacetogenesis has been observed under psychrophilic conditions, and some studies have reported that homoacetogens have a better ability to adapt to low temperatures than hydrogenotrophic methanogens (Kotsyurbenko *et al.*, 2001; Nozhevnikova *et al.*, 2003). No acetic acid accumulation (Fig. 1 presented as sum of VFA) was, however, observed at 15°C in this study. Competition between these groups did become apparent, when the temperature of

the reactors was reduced to 15°C, as indicated by the bacterial DGGE results (Fig. 2).

Sequence B21 was present in both systems, only after the transition to 15°C, and showed 99% similarity to *Acetobacterium carbinolicum* and *Acetobacterium psammolithicum* (phylum *Firmicutes*; Table 1). Both organisms were formerly described as psychro-active homoacetogenic bacteria, capable of growing at temperatures from 1°C to 35°C, with optimal growth between 20°C and 30°C (Conrad *et al*., 1989; Simankova *et al*., 2000). Enhanced activity of psychrotolerant homoacetogenic bacteria, followed by acetoclastic methanogenesis, has been previously reported to be important in the degradation of organic matter under low temperature conditions (Schulz and Conrad, 1996). There are also reports that homoacetogenic formation of acetate can bypass the formation of fatty acids and H_2, which could explain suppressed VFA production in our systems at 15°C, similar to that described for the decomposition of organic matter in anoxic paddy soil at low temperature (Chin and Conrad, 1995), or for the acidic sediment of Knaack Lake (Conrad *et al*., 1987). No increase in the maximum specific methanogenic activity with acetate as the substrate was noted with the biomass sampled from either reactors following the temperature decrease to 15°C (data not shown) and the quantitative analysis of methanogenic community structure did not record a large increase in acetoclastic methanogens (Fig. 4).

Phylogenetic analyses of the archaeal DGGE bands A1–A3 (Fig. 3B) indicated that hydrogen-utilizing *Methanocorpusculum*-like organisms (order *Methanomicrobiales*) were prominent after transition to low temperature. The *Methanocorpusculum*-like organisms deduced from A3 of the IFB system were likely to be the major hydrogenotrophic population in the low temperature reactor from day 365 (T3b, 15°C) onwards. In case of the EGSB reactor some part of the MMB population shifted towards *Methanospirillum*-like organisms deduced from A8 (T3a, 15°C) from day 298 onwards. Many studies have indeed documented that methanogenesis predominantly proceeded through the hydrogenotrophic route in low-temperature anaerobic reactors (Syutsubo *et al*., 2008; O'Reilly *et al*., 2009; McKeown *et al*., 2009a). In these situations, conditions with low hydrogen availability and high biomass concentration seemed to favour hydrogenotrophic methanogens due to their higher affinity for H_2 and thus they out-competed homoacetogens for hydrogen (Kotsyurbenko, 2005). It has been further proposed that hydrogen metabolism is thermodynamically and metabolically more favourable than acetate utilization; and that a higher level of hydrogen can be retained in the system (i.e. increased gas solubility) at low temperature (Lettinga *et al*., 2001; Kotsyurbenko, 2005). Supporting this, other authors (O'Reilly *et al*., 2009; McKeown *et al*., 2009a; Siggins *et al*., 2011) clearly demonstrated the temporal methanogenic community shifts towards the dominance of hydrogenotrophs, especially the order *Methanomicrobiales*, in low-temperature reactors compared with mesophilic systems. Hydrogenotrophic MMB showed a 1600- to 2200-fold increase in the 16S rRNA gene concentration from its minimum to maximum, corresponding to mesophilic and psychrophilic reactor operation in the IFB and EGSB reactors respectively (Fig. 4). Indeed, given this remarkable rise, low temperature appeared to be the major factor facilitating the emergence to dominance of this group in our reactors.

Experimental procedures

Reactor operation and biomass sampling

Replicate laboratory-scale IFB (IFB1 and IFB2) and EGSB (EGSB1 and EGSB2) reactors treating synthetic skimmed dairy wastewater (Table 3) were operated continuously for 430 days, in three periods (I to III) differentiated by operating temperature, from 37°C (period I, days 1–107), 25°C (period II, days 108–234) and 15°C (period III, days 235–430). This study is a continuation of the 200-day experiment at 37°C described in Bialek and colleagues (2011), thus a similar experimental approach has been employed to allow further comparison of the data. All reactors were operated at 24 h HRT, until day 294, when the HRT was changed to 48 h and further to 36 h on day 409. The performance of the reactors was evaluated on the basis of organic loading rate (OLR), chemical oxygen demand (COD), RE, EC and PRE. During periods I and II, the reactors were subjected to a fixed loading (OLR of 167 mg COD l^{-1} h^{-1} and HRT of 24 h) and during period III (15°C), the reactors were subjected to variable loading rates of 167, 83 and 111 mg COD l^{-1} h^{-1}, corresponding to 24, 48 and 36 h HRTs respectively. The length of each period was determined based on the stability of the reactor performance over time. RE, OLR and EC were calculated as described by Kumar and colleagues (2011).

For microbial community analysis, biomass samples were directly collected from each reactor at every temperature tested and designated accordingly for the duplicate IFB and EGSB reactors as: T1 (37°C, day 106); T2 (25°C, day 195); T3a (15°C, day 298), T3b (15°C, day 365); T3c (15°C, day 409), T3d (15°C, day 430). Biomass was sampled in duplicate (2×50 ml) and the estimated biomass concentration is provided in Table S1. Biomass for T1 and T2 was sampled during steady state and prior to changing operating conditions. During 15°C operation (T3), biomass was sampled more frequently to reflect the influence of operating and environmental conditions on the microbial community composition. Samples were first mechanically disrupted by manual grinding with a pestle and mortar and diluted 10-fold with deionized and distilled water prior to DNA extraction as described previously (Bialek *et al*., 2011). All DNA extractions were performed in duplicate.

Biomass samples collected directly from each reactor were also fixed for scanning electron microscopy analysis (SEM) using the protocol described by Katuri and colleagues (2010).

qPCR

Real-time PCR (qPCR) analysis was performed using a LightCycler 480 instrument (Roche, Mannheim, Germany). In this study qPCR analysis was performed using two methanogenic order-specific primer and probe sets: MBT, MMB, and two methanogenic family-specific primer and probe sets: Msc and Mst, which cover most methanogens in anaerobic digesters (Yu *et al*., 2005a,b; Lee *et al*., 2009). Methanogens are classified in five orders within the domain *Archaea* which can be grouped into two guilds, aceticlastic and hydrogenotrophic methanogens, determined by methane production pathways. Aceticlastic methanogens include only *Methanosarcinales*, which comprises two families, Mst utilizing only acetate and Msc utilizing acetate as well as various methyl compounds and hydrogen (Boone *et al*., 2001). Because those two aceticlastic methanogens play a crucial role in overall methanation (i.e. > 70% of methane is originated from acetate in most anaerobic systems) and the significant physiological differences between the two aceticlastic families (Hori *et al*., 2006; Yu *et al*., 2006), they were monitored at family level, instead of order level. Hydrogenotrophic methanogens comprise of four orders, i.e. MBT, *Methanococcales*, MMB and *Methanopyrales*, which utilize only $H_2 + CO_2$, formate or methanol to produce methane (Boone *et al*., 2001). Because the *Methanopyrales* members are not likely to be present in anaerobic processes due to their extremely high growth temperature (> 80°C) (Boone *et al*., 2001) and the members of *Methanococcales* are normally not found in anaerobic reactors, presumably since organisms from this group require high-salt conditions [0.3–9.4% (w/v) NaCl] for their growth (Boone *et al*., 2001), these two orders were left out of consideration in the present study. All DNA templates were analysed in duplicate. Quantitative standard curves were constructed using the representative strains corresponding to each primer and probe set, targeting the specific methanogenic groups (MBT, MMB, Msc, Mst), as described previously (Yu *et al*., 2005b; Bialek *et al*., 2011).

Statistical analysis

Non-metric multidimensional scaling was performed based on the real-time PCR results to visualize the quantitative shifts of methanogenic populations during reactor operation (McCune and Grace, 2002). The absolute quantity matrix of the target methanogenic groups detected by the qPCR assay (MBT, MMB, Msc and Mst) was created. Moving-window analysis was also carried out based on the absolute quantity matrix to monitor the variations in methanogenic community composition associated with decreases in the applied temperature of consecutive samplings in all reactors (Wittebolle *et al*., 2008; Bialek *et al*., 2011). The community similarity between two consecutive time points was used as the indicator of community variation in response to the corresponding temperature change. The Sørensen distance measure in the PC-ORD software ver. 5.0 (McCune and Grace, 2002) was employed for both analysis.

Archaeal and bacterial DGGE

Archaeal and bacterial 16S rRNA genes were amplified by PCR using the primer sets ARC GC 787F and ARC 1059R (Takai and Horikoshi, 2000), BAC GC 338F and BAC805 R (Yu *et al*., 2005a,b) respectively. Touchdown PCR, PCR products purification, sequencing, sequencing alignment and phylogenetic analyses were performed as described previously (Bialek *et al*., 2011). DNA from DGGE experiments were sequenced in Germany by Eurofins MWG Operon. Phylogeny was calculated using the neighbour-joining method (Saitou and Nei, 1987). Bacterial distances were computed using the maximum composite likelihood method (Tamura *et al*., 2004) and archaeal distances were computed using the Kimura 2-parameter method (Kimura, 1980) and are in the units of the number of base substitutions per site. The bootstrap consensus trees inferred from 1000 replicates are taken to represent the evolutionary history of the taxa analysed (Felsenstein, 1985).

The UPGMA (McCune and Grace, 2002) was selected to perform statistical analysis of the DGGE profiles. The scanned DGGE gel image was processed with Phoretix 1D (previously TotalLab TL120 software; TotalLab, Newcastle upon Tyne, UK) to construct a binary matrix, where the presence or absence of each band was scored with 1 or 0, respectively, without considering band intensity. Construction of the dendogram via hierarchical clustering was performed based on the Sørensons (Bray–Curtis) distance measurement using MEGA 4 software (Tamura *et al*., 2007).

All nucleotide sequence data reported in this study were deposited in the GenBank database under accession numbers ARC: JF952003–JF952011 and BAC: JF927800–JF927829.

Analytical analysis

Biogas and effluent from all reactors were sampled every second day to analyse respectively, the biogas methane content and residual effluent COD concentration according to standard methods (APHA, 2005). Analysis of effluent VFA were performed in a Varian Saturn 2000 GC/MS system, with CombiPAL autosampler (Varian, Walnut Creek, CA) as described previously (Bialek *et al*., 2011). Total protein quantification in the effluent samples was performed using the *RC DC* protein assay kit (Bio-Rad). All analyses were performed in duplicate.

Acknowledgements

This research was carried out with the financial support of Science Foundation Ireland (Charles Parsons Energy Research Award – 06/CP/E006). The award of an Embark Scholarship to K. Bialek by the Irish Research Council for Science, Engineering and Technology is also gratefully acknowledged. Valuable scientific discussions with Denise Cysneiros are gratefully acknowledged.

References

Allison, S.D., and Martiny, J.B.H. (2008) Resistance, resilience, and redundancy in microbial communities. *Proc Natl Acad Sci USA* **105:** 11512–11519.

Alvarado-Lassman, A., Rustrián, E., García-Alvarado, M.A., Rodríguez-Jiménez, G.C., and Houbron, E. (2008)

Brewery wastewater treatment using anaerobic inverse fluidized bed reactors. *Bioresour Technol* **99:** 3009–3015.
APHA (2005) *Standard Methods for the Examination of Water and Wastewater*, 21st edn. AWWA (ed.). Washington, DC: APHA-AWWA-WEF.
Bergamo, C.M., Di Monaco, R., Ratusznei, S.M., Rodrigues, J.A.D., Zaiat, M., and Foresti, E. (2009) Effects of temperature at different organic loading levels on the performance of a fluidized-bed anaerobic sequencing batch bioreactor. *Chem Eng Process* **48:** 789–796.
Bialek, K., Kim, J., Lee, C., Collins, G., Mahony, T., and O'Flaherty, V. (2011) Quantitative and qualitative analyses of methanogenic community development in high-rate anaerobic bioreactors. *Water Res* **45:** 1298–1308.
Boone, D.R., Castenholz, R.W., and Garrity, G.M. (2001) Bergey's manual of systematic bacteriology. In *The Archaea and the Deeply Branching and Phototrophic Bacteria Volume 1***.** New York, NY: Springer-Verlag New York, Inc.
Briones, A., and Raskin, L. (2003) Diversity and dynamics of microbial communities in engineered environments and their implications for process stability. *Curr Opin Biotechnol* **14:** 270–276.
Carballa, M., Smits, M., Etchebehere, C., Boon, N., and Verstraete, W. (2011) Correlations between molecular and operational parameters in continuous lab-scale anaerobic reactors. *Appl Microbiol Biotechnol* **89:** 303–314.
Chin, K.J., and Conrad, R. (1995) Intermediary metabolism in methanogenic paddy soil and the influence of temperature. *FEMS Microbiol Ecol* **18:** 85–102.
Collins, G., Woods, A., McHugh, S., Carton, M.W., and O'Flaherty, V. (2003) Microbial community structure and methanogenic activity during start-up of psychrophilic anaerobic digesters treating synthetic industrial wastewaters. *FEMS Microbiol Ecol* **46:** 159–170.
Collins, G., Kavanagh, S., McHugh, S., Connaughton, S., Kearney, A., Rice, O., *et al*. (2006) Accessing the black box of microbial diversity and ecophysiology: recent advances through polyphasic experiments. *J Environ Sci Health A Tox Hazard Subst Environ Eng* **41:** 897–922.
Conrad, R., Goodwin, S., and Zeikus, J. (1987) Hydrogen metabolism in a mildly acidic lake sediment (Knaack Lake). *FEMS Microbiol Lett* **45:** 243–249.
Conrad, R., Bak, F., Seitz, H., Thebrath, B., Mayer, H., and Schütz, H. (1989) Hydrogen turnover by psychrotrophic homoacetogenic and mesophilic methanogenic bacteria in anoxic paddy soil and lake sediment. *FEMS Microbiol Lett* **62:** 285–293.
Demirel, B., Scherer, P., Yenigun, O., and Onay, T.T. (2010) Production of methane and hydrogen from biomass through conventional and high-rate anaerobic digestion processes. *Crit Rev Environ Sci and Tech* **40:** 116–146.
Fang, H.H.P., and Yu, H.Q. (2000) Effect of HRT on mesophilic acidogenesis of dairy wastewater. *J Environ Eng* **126:** 1145–1148.
Felsenstein, J. (1985) Confidence-limits on phylogenies – an approach using the Bootstrap. *Evolution* **39:** 783–791.
Garcia-Calderon, D., Buffiere, P., Moletta, R., and Elmaleh, S. (1998) Anaerobic digestion of wine distillery wastewater in down-flow fluidized bed. *Water Res* **32:** 3593–3600.
Grotenhuis, J.T., Smit, M., Plugge, C.M., Xu, Y.S., van Lammeren, A.A., Stams, A.J., and Zehnder, A.J. (1991) Bacteriological composition and structure of granular sludge adapted to different substrates. *Appl Environ Microbiol* **57:** 1942–1949.
Hashsham, S.A., Fernandez, A.S., Dollhopf, S.L., Dazzo, F.B., Hickey, R.F., Tiedje, J.M., and Criddle, C.S. (2000) Parallel processing of substrate correlates with greater functional stability in methanogenic bioreactor communities perturbed by glucose. *Appl Environ Microbiol* **66:** 4050–4057.
Hori, T., Haruta, S., Ueno, Y., Ishii, M., and Igarashi, Y. (2006) Dynamic transition of a methanogenic population in response to the concentration of volatile fatty acids in a thermophilic anaerobic digester. *Appl Environ Microbiol* **72:** 1623–1630.
Katuri, K.P., Kavanagh, P., Rengaraj, S., and Leech, D. (2010) Geobacter sulfurreducens biofilms developed under different growth conditions on glassy carbon electrodes: insights using cyclic voltammetry. *Chem Commun* **46:** 4758–4760.
Kimura, M. (1980) A simple method for estimating evolutionary rates of base substitutions through comparative studies of nucleotide sequences. *J Mol Evol* **16:** 111–120.
Kotsyurbenko, O.R. (2005) Trophic interactions in the methanogenic microbial community of low-temperature terrestrial ecosystems. *FEMS Microbiol Ecol* **53:** 3–13.
Kotsyurbenko, O.R., Glagolev, M.V., Nozhevnikova, A.N., and Conrad, R. (2001) Competition between homoacetogenic bacteria and methanogenic archaea for hydrogen at low temperature. *FEMS Microbiol Ecol* **38:** 153–159.
Kumar, A., Lens, P., Ergas, S., and Van Langenhove, H. (2011) *Reactors for Waste Gas Treatment: Principles, Process Engineering, Performance and Development Requirements*. New York, USA: Taylor & Francis.
Lee, C., Kim, J., Hwang, K., O'Flaherty, V., and Hwang, S. (2009) Quantitative analysis of methanogenic community dynamics in three anaerobic batch digesters treating different wastewaters. *Water Res* **43:** 157–165.
Lettinga, G., Rebac, S., Parshina, S., Nozhevnikova, A., van Lier, J.B., and Stams, A.J. (1999) High-rate anaerobic treatment of wastewater at low temperatures. *Appl Environ Microbiol* **65:** 1696–1702.
Lettinga, G., Rebac, S., and Zeeman, G. (2001) Challenge of psychrophilic anaerobic wastewater treatment. *Trends Biotechnol* **19:** 363–370.
Lovley, D.R., and Klug, M.J. (1983) Methanogenesis from methanol and methylamines and acetogenesis from hydrogen and carbon dioxide in the sediments of a eutrophic lake. *Appl Environ Microbiol* **45:** 1310–1315.
McCune, B., and Grace, J.B. (2002) *Analysis of Ecological Communities*. MjM Software Design: Gleneden Beach, OR.
McHugh, S., Carton, M., Collins, G., and O'Flaherty, V. (2004) Reactor performance and microbial community dynamics during anaerobic biological treatment of wastewaters at 16–37 degrees C. *FEMS Microbiol Ecol* **48:** 369–378.
McKeown, R.M., Scully, C., Enright, A.M., Chinalia, F.A., Lee, C., Mahony, T., *et al*. (2009a) Psychrophilic methanogenic community development during long-term cultivation of anaerobic granular biofilms. *ISME J* **3:** 1231–1242.

McKeown, R.M., Scully, C., Mahony, T., Collins, G., and O'Flaherty, V. (2009b) Long-term (1243 days), low-temperature (4–15 degrees C), anaerobic biotreatment of acidified wastewaters: bioprocess performance and physiological characteristics. *Water Res* **43:** 1611–1620.

McKeown, R.M., Hughes, D., Collins, G., Mahony, T., and O'Flaherty, V. (2012) Low-temperature anaerobic digestion for wastewater treatment. *Curr Opin Biotechnol* **23:** 444–451.

Madden, P., Chinalia, F.A., Enright, A.M., Collins, G., and O'Flaherty, V. (2010) Perturbation-independent community development in low-temperature anaerobic biological wastewater treatment bioreactors. *Biotechnol Bioeng* **105:** 79–87.

Nelson, M.C., Morrison, M., and Yu, Z. (2011) A meta-analysis of the microbial diversity observed in anaerobic digesters. *Bioresour Technol* **102:** 3730–3739.

Nozhevnikova, A.N., Zepp, K., Vazquez, F., Zehnder, A.J., and Holliger, C. (2003) Evidence for the existence of psychrophilic methanogenic communities in anoxic sediments of deep lakes. *Appl Environ Microbiol* **69:** 1832–1835.

O'Reilly, J., Lee, C., Collins, G., Chinalia, F., Mahony, T., and O'Flaherty, V. (2009) Quantitative and qualitative analysis of methanogenic communities in mesophilically and psychrophilically cultivated anaerobic granular biofilims. *Water Res* **43:** 3365–3374.

Perle, M., Kimchie, S., and Shelef, G. (1995) Some biochemical aspects of the anaerobic degradation of dairy wastewater. *Water Res* **29:** 1549–1554.

Raes, J., and Bork, P. (2008) Molecular eco-systems biology: towards an understanding of community function. *Nat Rev Microbiol* **6:** 693–699.

Saitou, N., and Nei, M. (1987) The neighbor-joining method – a new method for reconstructing phylogenetic trees. *Mol Biol Evol* **4:** 406–425.

Schulz, S., and Conrad, R. (1996) Influence of temperature on pathways to methane production in the permanently cold profundal sediment of Lake Constance. *FEMS Microbiol Ecol* **20:** 1–14.

Siggins, A., Enright, A.M., and O'Flaherty, V. (2011) Temperature dependent (37–15 degrees C) anaerobic digestion of a trichloroethylene-contaminated wastewater. *Bioresour Technol* **102:** 7645–7656.

Simankova, M.V., Kotsyurbenko, O.R., Stackebrandt, E., Kostrikina, N.A., Lysenko, A.M., Osipov, G.A., and Nozhevnikova, A.N. (2000) *Acetobacterium tundrae* sp. nov., a new psychrophilic acetogenic bacterium from tundra soil. *Arch Microbiol* **174:** 440–447.

Syutsubo, K., Yoochatchaval, W., Yoshida, H., Nishiyama, K., Okawara, M., Sumino, H., *et al*. (2008) Changes of microbial characteristics of retained sludge during low-temperature operation of an EGSB reactor for low-strength wastewater treatment. *Water Sci Technol* **57:** 277–281.

Takai, K., and Horikoshi, K. (2000) Rapid detection and quantification of members of the archaeal community by quantitative PCR using fluorogenic probes. *Appl Environ Microbiol* **66:** 5066–5072.

Talbot, G., Topp, E., Palin, M.F., and Massé, D.I. (2008) Evaluation of molecular methods used for establishing the interactions and functions of microorganisms in anaerobic bioreactors. *Water Res* **42:** 513–537.

Tamura, K., Nei, M., and Kumar, S. (2004) Prospects for inferring very large phylogenies by using the neighbor-joining method. *Proc Natl Acad Sci USA* **101:** 11030–11035.

Tamura, K., Dudley, J., Nei, M., and Kumar, S. (2007) MEGA4: molecular evolutionary genetics analysis (MEGA) software version 4.0. *Mol Biol Evol* **24:** 1596–1599.

Tommaso, G., Ribeiro, R., Varesche, M.B., Zaiat, M., and Foresti, E. (2003) Influence of multiple substrates on anaerobic protein degradation in a packed-bed bioreactor. *Water Sci Technol* **48:** 23–31.

Verstraete, W., and Gusseme, B. (2011) Crystal ball: visions about water and sanitation for the cities of the future: time to rethink environmental microbial processes. *Microbial Biotechnol* **4:** 109–137.

Wendeberg, A., Zielinski, F.U., Borowski, C., and Dubilier, N. (2012) Expression patterns of mRNAs for methanotrophy and thiotrophy in symbionts of the hydrothermal vent mussel *Bathymodiolus puteoserpentis*. *ISME J* **6:** 104–112.

Werner, J.J., Knights, D., Garcia, M.L., Scalfone, N.B., Smith, S., Yarasheski, K., *et al*. (2011) Bacterial community structures are unique and resilient in full-scale bioenergy systems. *Proc Natl Acad Sci USA* **108:** 4158–4163.

Wittebolle, L., Vervaeren, H., Verstraete, W., and Boon, N. (2008) Quantifying community dynamics of nitrifiers in functionally stable reactors. *Appl Environ Microbiol* **74:** 286–293.

Yu, Y., Lee, C., and Hwang, S. (2005a) Analysis of community structures in anaerobic processes using a quantitative real-time PCR method. *Water Sci Technol* **52:** 85–91.

Yu, Y., Lee, C., Kim, J., and Hwang, S. (2005b) Group-specific primer and probe sets to detect methanogenic communities using quantitative real-time polymerase chain reaction. *Biotechnol Bioeng* **89:** 670–679.

Yu, Y., Kim, J., and Hwang, S. (2006) Use of real-time PCR for group-specific quantification of aceticlastic methanogens in anaerobic processes: population dynamics and community structures. *Biotechnol Bioeng* **93:** 424–433.

Zumstein, E., Moletta, R., and Godon, J.J. (2000) Examination of two years of community dynamics in an anaerobic bioreactor using fluorescence polymerase chain reaction (PCR) single-strand conformation polymorphism analysis. *Environ Microbiol* **2:** 69–78.

Supporting information

Additional Supporting Information may be found in the online version of this article:

Fig. S1. Reactor configuration and zoom in showing scanning electron microscopy (SEM) images of the biofilm biomass from (A) the inverted fluidized bed (IFB) and (B) expanded granular sludge bed (EGSB) reactors.

Table S1. Evaluation of biomass concentration in the reactors over the 430-day trial.

Please note: Wiley-Blackwell are not responsible for the content or functionality of any supporting materials supplied by the authors. Any queries (other than missing material) should be directed to the corresponding author for the article.